BIOLOGY OF REPRODUCTION (2015) **93**(4):88, 1–10
Published online before print 5 August 2015.
DOI 10.1095/biolreprod.115.131227

Geography of Follicle Formation in the Embryonic Mouse Ovary Impacts Activation Pattern During the First Wave of Folliculogenesis[1]

Marília H. Cordeiro,[3,4,5] So-Youn Kim,[3] Katherine Ebbert,[3] Francesca E. Duncan,[3] João Ramalho-Santos,[4,6] and Teresa K. Woodruff[2,3]

[3]*Department of Obstetrics and Gynecology, Feinberg School of Medicine, Northwestern University, Chicago, Illinois*
[4]*Center for Neuroscience and Cell Biology, University of Coimbra, Coimbra, Portugal*
[5]*Doctoral Programme in Experimental Biology and Biomedicine, Center for Neuroscience and Cell Biology, University of Coimbra, Coimbra, Portugal*
[6]*Department of Life Sciences, University of Coimbra, Coimbra, Portugal*

ABSTRACT

During embryonic development, mouse female germ cells enter meiosis in an anterior-to-posterior wave believed to be driven by retinoic acid. It has been proposed that ovarian follicle formation and activation follow the same general wave of meiotic progression; however, the precise anatomic specification of these processes has not been delineated. Here, we created a mouse line using *Mvh*, *Gdf9,* and *Zp3* promoters to drive distinct temporal expression of three fluorescent proteins in the oocytes and to identify where the first follicle cohort develops. The fluorescent profile revealed that the first growing follicles consistently appeared in a specific region of the ovary, the anterior-dorsal region, which led us to analyze if meiotic onset occurred earlier in the dorsal ovarian region. Surprisingly, in addition to the anterior-to-posterior wave, we observed an early meiotic entry in the ventral region of the ovary. This additional anatomic stratification of meiosis contrasts with the localization of the initial follicle formation and activation in the dorsal region of the ovary. Therefore, our study suggests that the specification of cortical and medullar areas in the ventral and dorsal regions on the ovary, rather than the onset of meiosis, impacts where the first follicle activation event occurs.

follicle activation, follicle formation, meiosis, ovarian geography, ovary

INTRODUCTION

Normal ovarian function throughout the mammalian reproductive life span requires tight regulation between germ cell arrest, differentiation, and loss at the time of gonadal development and within each reproductive cycle. The size of the ovarian germ cell pool changes during development, achieving its maximum number as the primordial germ cells (PGCs) colonize the gonad and undergo mitotic divisions [1, 2]. In mouse, the female germ cells undergo meiosis around 13.5 days postcoitum (dpc), which occurs in an anterior-to-posterior wave driven by retinoic acid, whereas the male germ cells only undergo meiosis after birth [3–6]. Female germ cells arrest at prophase I, grouped into cell clusters connected by intercellular bridges. These germ cell ''cysts'' undergo a process of nest breakdown, resulting in individual primordial follicle formation due to invasion of pregranulosa cells or germ cell loss [7]. During the estrous cycle, a small number of primordial follicles are activated to grow and, under hormonal control, release a mature oocyte. Because follicle activation is irreversible and the starting pool of follicles is finite, the size of the ovarian reserve is gradually reduced, in turn defining the female reproductive life span [1, 2].

The mechanism by which a particular follicle is selected to grow while others remain dormant is still not fully understood. Genetically modified animals have been extremely valuable to identify molecules and signaling pathways involved in global primordial follicle activation and survival (for reviews, see [8, 9]); however, the trigger for individual follicle activation at different times remains unknown. The ''production line'' hypothesis is a popular proposition to explain the order of activation. This hypothesis, originally proposed to justify the high incidence of aneuploidy in reproductively aged females, suggests that the first oogonia to undergo meiotic arrest are also the first to become activated after puberty, implying that the order of follicle activation is established during embryonic development [10]. However, this hypothesis has remained controversial, with evidence in favor [11–13] and against [14–18]. In support of the production line hypothesis, follicle formation progresses gradually from the medulla to the cortex, with the germ cells closest to the medulla becoming the first follicles to be formed and activated [19–21]. It has been accepted that the first growing follicles—the first wave of follicle activation—reach the antral stage before puberty in the absence of gonadotropin regulation and therefore are lost by atresia [22]. However, a recent study suggested that these first-wave follicles not only induce the onset of puberty but also are ovulated, growing faster than follicles activated in the adult ovary [23]. On the other hand, pregranulosa cells arise from the surface epithelium in two waves: an initial fetal wave integrated

[1]Supported by the Eunice Kennedy Shriver National Institute of Child Health and Human Development of the National Institutes of Health (P50HD076188 and P01HD021921). Additional support was provided by the Thomas J. Watkins Professor of Obstetrics and Gynecology Endowment at Northwestern University and the Portuguese PhD Fellowship from Fundação para a Ciência e Tecnologia (FCT) to M.H.C. (SFRH/BD/33886/2009). Presented in part at the 47th Annual Meeting of the Society for the Study of Reproduction, July 19–23, 2014, Grand Rapids, Michigan, and the 16th International Congress of Endocrinology & the Endocrine Society's 96th Annual Meeting & Expo, June 21–24, 2014, Chicago, Illinois.
[2]Correspondence**:** Teresa K. Woodruff, Northwestern University Feinberg School of Medicine, Department of Obstetrics and Gynecology, 303 East Superior Street, Lurie Building 10-121, Chicago, IL 60611. E-mail: tkw@northwestern.edu

Received: 30 April 2015.
First decision: 20 May 2015.
Accepted: 4 August 2015.

eISSN: 1529-7268 http://www.biolreprod.org
ISSN: 0006-3363

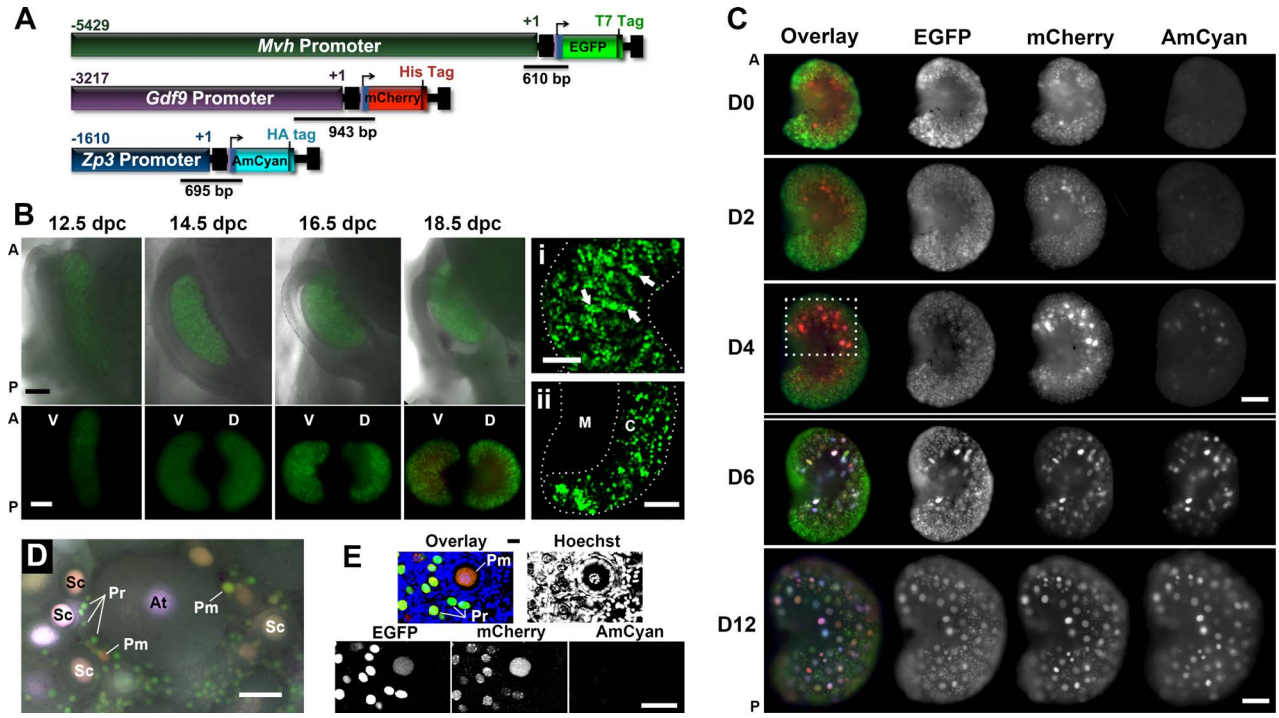

FIG. 1. Expression of the fluorescent proteins changed according to the developmental stage of the germ cell. **A**) Map of the linear constructs used to generate the triple-transgenic line and design of the genotyping primers. **B**) Expression of reporter proteins during embryonic development (epifluorescence). **Top**) Anatomic changes of the ovary and reproductive tract. **Bottom**) Ventral (V) and dorsal (D) regions of the same ovary, rotated horizontally. A, anterior; P, posterior. Bar = 200 μm. Detail of the cord-like structures (i; arrows highlight germ cell cluster) and specification of a medullar region (ii) in 18.5-dpc ovaries (confocal maximum projections) are shown. M, medulla; C, cortex. Bar in i and ii = 100 μm. **C**) Fluorescent protein expression in the dorsal ovarian region of different age mouse (epifluorescence). Dashed box highlights the ovarian area where follicles first grow. Different imaging settings were used at D0 to D4 and D6 to D12. A higher EGFP and lower AmCyan and mCherry exposure times were used on D6 and D12 to avoid saturation of the images. Bar = 200 μm. **D**) Representative follicles in the surface of the ventral region in a 16-day-old mouse ovary (epifluorescence). Follicle stage was determined based on the follicular morphology in the bright-field image. Pr, primordial; Pm, primary; Sc, secondary; At, antral. Bar = 50 μm. **E**) Small follicles in a 16-day-old mouse ovary (confocal). Primordial follicles (Pr) only express EGFP and mCherry at various levels. DNA probe Hoechst 33342 was used to determine follicle class. Bar = 50 μm.

into medullary follicles, which initiate growth shortly after birth, and a neonatal wave that surrounds cortical follicles, resulting in distinct follicle fates [24]. Furthermore, at the time of individual follicle formation, granulosa cells undergo mitotic arrest, which may control the rate of follicle activation [12, 24]. As described above, major differences have been identified in germ and somatic cell dynamics between follicles from the first and consecutive waves of activation, but to our knowledge, no published studies have analyzed in detail how and where the first wave of activation is established in the mouse ovary.

Although several mouse lines have been generated to label the germ cells at a specific time of ovarian and/or follicle development [25, 26], we lack a reporter line able to dynamically represent the developmental progression of the ovarian follicle. Thus, the present study aims, first, to create a tool to examine follicle development in vivo and in vitro and, second, to use this mouse line to explore the role of ovarian anatomy in establishment of the first wave of follicle activation in an effort to further elaborate on the production line hypothesis and determine how selective primordial recruitment occurs during the first wave of folliculogenesis.

MATERIALS AND METHODS

Mvh/Gdf9/Zp3 *DNA Constructs*

The three DNA linear fragments containing *Mvh*, *Gdf9*, and *Zp3* promoters were built into a *Zp3* cassette plasmid [27] by engineering the promoter and fluorescent protein regions. EGFP (enhanced green fluorescent protein), mCherry, and AmCyan were amplified from the plasmids *Zp3* cassette, pIVT+NtermCherry (both generously provided by Dr. Richard M. Schultz, University of Pennsylvania, Philadelphia, PA), and pAmCyan1-N1 (Clontech), respectively. New restriction sites and epitope tags (HA, His, and T7 tags to ensure reporter detection) were engineered into the 5′ ends of the primers. *Gdf9* promoter was obtained from the pGDF9-Luc vector [26] (generously provided by Dr. Austin J. Cooney, Baylor College of Medicine, Houston, TX), and *Mvh* promoter sequence was amplified from pVASA-creN vector [28] (provided by Dr. Diego H. Castrillon, University of Texas Southwestern Medical Center, Dallas, TX, through Addgene). Sequencing was used to confirm correct construct building (performed by Northwestern University Genomics Core, Chicago, IL). Further details can be found in the Supplemental Materials and Methods and in Supplemental Table S1 (all Supplemental Data are available online at www.biolreprod.org).

Generation of the Triple Transgenic Mice and Animal Care

The linear DNA fragments *Zp3*-AmCyan-HA (2886 bp), *Mvh*-EGFP-T7 (6694 bp), and *Gdf9*-mCherry-His (4471 bp) were coinjected at equimolar ratios into 1-cell-embryos from adult CD-1 mice (Crl:CD1[(ICR]; Charles River), using standard protocols (performed at Northwestern University Transgenic Facility, Chicago, IL) (Fig. 1A). Details on screening of founder lines can be found in Supplemental Figure S1, Supplemental Table S2, and the Supplemental Materials and Methods. All procedures involving mice were approved by the Northwestern University Animal Care and Use Committee. Mice were housed and bred in a barrier facility within Northwestern University's Center of Comparative Medicine (Chicago, IL) and were provided with food and water ad libitum. Temperature, humidity, and photoperiod (14L:10D) were kept constant.

Genotyping

The genotype was assessed by PCR using the following primers: *Gdf9*-mCherry (F1, 5′-TCAAAATTATGTAGCTCTGACTGTCC-3′; R1, 5′-

CCCTCCATGTGCACCTTGAAGCGCAT-3′), *Zp3*-AmCyan (F2, 5′-AGAGTTACACTGAGAAATCCTGCCC; R2, 5′-CCTCGCCCTTCACGGT GAAGTAGTG), and *Mvh*-EGFP (F3, 5′-ACGTGCAGCCGTTTAAGCCG-3′; R3, 5′-TTGCCGTCGTCCTTGAAGAA-3′) (Supplemental Table S1). The primers were designed to originate a PCR product that contains part of the promoter sequence and part of the fluorescent protein, therefore detecting the functional unit of the transgenes (denoted in Fig. 1A). The different transgenes were distinguished by the size of the PCR product and detected as 943-, 695-, and 610-bp products, respectively. The PCR conditions were 94°C for 5 min, followed by 40 cycles of 94°C for 45 sec, 56°C (*Gdf9*-mCherry and *Zp3*-AmCyan) or 60°C (*Mvh*-EGFP) for 45 sec, and 72°C for 1 min, with a final step of 72°C for 2 min.

Timed Pregnancy and Embryo Collection

Vaginal cytology was used to follow estrous cycles as previously described [29]. Wild-type CD-1 females on proestrus were housed overnight with a transgenic male and separated into single cages the next morning to ensure accurate timing of pregnancy. Noon of plug detection day was considered to be Embryonic Day 0.5. Embryos were collected in L15 medium containing 10% fetal bovine serum (FBS; Life Technologies) and dissected as previously described [30]. Briefly, embryos were removed from their extraembryonic membranes and cut below the armpits and along the ventral midline of the posterior half of the embryo. Internal organs were removed with fine forceps, allowing visualization of the genital ridges lying on the dorsal wall of the embryos. To image the embryonic ovaries in their native orientation, the embryos were placed ventrally against the dish and visualized using a Nikon Eclipse Ti epifluorescent inverted microscope.

Ovary Collection and Imaging

The day of birth was counted as Postnatal Day 0. Ovaries were collected and dissected from the bursa in L15 medium containing penicillin-streptomycin and 10% FBS. Embryonic and postnatal ovaries were imaged immediately after collection on a Nikon Eclipse Ti epifluorescent microscope using C-FL CFP 96341 (AmCyan), C-FL YFP BP HYQ 96345 (EGFP), and C-FL Y-2E/C Texas Red 96313 (mCherry) cubes from Nikon. The yellow fluorescent protein (YFP) cube was used to detect EGFP to minimize cross-detection of AmCyan because the two fluorescent proteins have similar spectral properties. The detection of EGFP using the YFP cube is not optimal because it limits the tail of the fluorescence spectrum; this explains why the EGFP signal appears relatively weak on the epifluorescence images. Confocal images were acquired on a Nikon A1R Laser Resonant Scanning Confocal Microscope using the laser lines 457 (AmCyan), 488 (EGFP), and 561 (mCherry) (Northwestern University Cell Imaging Facility). Cross-detection of the distinct fluorescent proteins is minimized by the imaging settings but cannot be excluded in any of the imaging systems used. Z-stack images of the ovaries were collected from the first layer of cells on the surface of the ovary until no signal could be detected. Three-dimensional maximum projection reconstructions of the z-stacks were created on Nikon Elements NIS software. For all ages, oocytes located within 80 μm of depth are represented in the maximum projections, corresponding to the maximum penetration of the laser at the imaging settings used. The ovaries were kept intact during live imaging. Ventral and dorsal regions of the same ovary were imaged by rotating the ovary horizontally using a blunted pipette tip. When needed, ovaries were incubated with the DNA probe Hoechst 33342 (10 μg/ml; Life Technologies) for 5 min at 37°C, allowing identification of granulosa cell shape and the number of layers. Follicles were classified according to their morphologic features [31]. Follicles surrounded by a single layer of flattened granulosa cells were considered to be primordial follicles. In the whole-ovary images, the fluorescent signal of the germ cell was used to help identify the follicle class and was confirmed by analyzing the bright-field image collected simultaneously. All the tissue used for live imaging was discarded and not used for further analysis. Live imaging was the preferred method because the fluorescent signal in this transgenic line is relatively weak compared with other reporter lines using Rosa26 or actin locus to drive reporter proteins. The fluorescence is dramatically decreased after fixation with 4% paraformaldehyde and deleted by Modified Davison fixative (Electron Microscopy Sciences). Additionally, the autofluorescence of the background increased with the fixation process, and the commercially available clearing solution that was tested only slightly improve the image.

Histological Analysis and Immunohistochemistry

Embryonic and postnatal mouse ovaries from transgenic mice and wild-type siblings were fixed with Modified Davison fixative overnight (embryonic ovaries) and 24 h (postnatal ovaries) at 4°C. Tissue was then included in an alginate disk before being processed and embedded in paraffin. The inclusion in alginate disks allowed sectioning of the tissue with a specific orientation. Briefly, fixed ovaries were placed in top of a 0.4-μm-pore insert (Millipore) and covered with 2% alginate diluted in Ca^{2+}/Mg^{2+}-free PBS. Ovaries were oriented, with the ventral ovarian region facing against the membrane, using insulin needles and allowed to crosslink overnight at 4°C in 4% paraformaldehyde-Ca^{2+}-cacodylate solution. The surface of the disk was stained with alcian blue to facilitate orientation during embedding. The embryonic tissue was not dissected from the mesonephros to facilitate orientation of the gonads. Ovarian tissue was serially sectioned (thickness, 5 μm) from the ventral to the dorsal face of the ovary. Dorsal and ventral regions were defined as the outermost sections containing germ cells. Hematoxylin-and-eosin staining was performed using standard methods.

Immunofluorescence assay was performed as previously described [32, 33] with some modifications. Briefly, after deparaffinization and rehydration of the ovarian sections, antigen retrieval was performed using freshly made sodium citrate buffer (10 mM sodium citrate and 0.05% Tween-20, pH 6.0) in a pressure cooker for 40 min. Slides were incubated with 3% hydrogen peroxide in Tris-buffered saline for 15 min, followed by incubation with Avidin-Biotin Blocking Kit (Vector Laboratories) according to manufacturer's instructions and blocking for 1 h at room temperature with blocking solution (2% donkey serum, 1% bovine serum albumin, 0.1% cold fish skin gelatin, 0.1% Triton X-100, 0.05% Tween-20, and 0.05% sodium azide in 0.01 M PBS). Sections were incubated overnight at 4°C with primary antibodies: HA tag (1:200; H6908; Sigma-Aldrich), MVH (Mouse Vasa Homolog; 1:50; DDX4/MVH antibody; ab138440; Abcam), OCT4 (octamer-binding protein 4, POU5F1, 1:50; P0056; Sigma-Aldrich); STRA8 (stimulated by retinoic acid 8, 1:50; ab49602; Abcam), FOXL2 (forkhead box L2, 1:50; ab5096; Abcam), laminin (1:100; L9393; Sigma-Aldrich), and p63 (1:100; sc-8431; Santa Cruz Biotechnology). Signals were amplified using biotinylated secondary antibodies against rabbit (Jackson ImmunoResearch) and goat (Vector Laboratories), followed by VECTASTAIN ABC Kit (PK-6100; Vector Laboratories) and TSA Plus Fluorescein System (1:400 dilution for 1 min; PerkinElmer). Laminin and p63 antibodies did not require amplification; thus, fluorophore-conjugated secondary antibody was used instead (anti-rabbit Alexa Fluor 488 and anti-mouse Alexa Fluor 594; both from Jackson ImmunoResearch). Slides were mounted with VECTASHIELD containing 4′,6-diamidino-2-phenylindole (DAPI; Vector Laboratories) to visualize the nucleus and imaged using a Nikon Eclipse E600 microscope. The specificity of signals was confirmed with a negative control in which the primary antibody was omitted. Three to five animals from three independent litters (total of 9–15 independent ovaries) were analyzed per each developmental time point. Follicles were classified according to standard morphologic criteria [31].

RESULTS

Oocyte-Specific Fluorescent Protein Expression Did Not Alter Reproductive Function

To generate a reporter line to dynamically follow follicle activation and growth, we used the oocyte-specific promoters *Mvh*, *Gdf9,* and *Zp3* to drive the expression of the fluorescent proteins EGFP, mCherry, and AmCyan, respectively (Fig. 1A). These well-characterized promoters are active at distinct stages of follicle development and have been used routinely to create oocyte-specific knockouts (see, e.g., [26, 28, 34–37]). In the mouse ovary, MVH (mouse vasa homolog, VASA, DDX4) expression begins as PGCs migrate and colonize the gonad, and it is highly expressed in primordial follicles and decreases with follicle development [38, 39]. GDF9 (growth differentiation factor 9) is critical for early and late stages of folliculogenesis, with a somewhat controversial onset of expression at the primordial follicle stage and continuing in later developmental stages as well [26, 40, 41]. ZP3 (zona pellucida glycoprotein 3) expression is first detected in primary follicles, reaching its maximum in growing follicles and decreasing in fully grown oocytes [42, 43]. Therefore, we expected that the temporal difference in activity of these promoters would result in an oocyte fluorescence signature able to provide readout of follicle activation and maturation.

Pronuclear injection resulted in the generation of nine transgenic founders, one double- and eight triple-transgenic animals (Supplemental Fig. S1 and Supplemental Table S2).

Each founder line had a unique segregation pattern and expression level, likely related to differences in integration site and copy number of the transgenes [30]. Promoter specificity was observed, with fluorescent protein expression restricted to the female and male germ cells (Supplemental Figs. S2 and S3). A single founder line was selected based on the high expression levels of the three fluorescent proteins and cosegregation of the transgenes over four generations (Supplemental Fig. S1 and Table S2). This mouse line showed normal fertility, confirming that the transgenes did not interfere with reproductive function (Supplemental Fig. S2C).

Transgene Profile Reflects Germ Cell Development

To determine if the fluorescent protein expression in the transgenic mice reflected follicle development and ovarian physiology, we performed live imaging of whole ovaries from mice of different ages (Fig. 1, B and C). As expected, based on the timing of expression described for the endogenous promoters, EGFP driven by the *Mvh* promoter (*Mvh*-EGFP) was the only fluorescent protein detected in the germ cells during the embryonic period (Fig. 1B). This reporter protein, expressed at low levels during early gonadal development, revealed key anatomic and cellular events during early development, including changes in gonadal shape and establishment of germ cell clusters organized in cord-like structures visible at 14.5 dpc (Fig. 1B bottom panel and Fig. 1Bi). By 16.5 dpc, the specification of a medullar region was prominent in the dorsal side of the ovary, as evidenced by the absence of germ cells in this region (Fig. 1B bottom panel and Fig. 1Bii). Significant changes in the anatomic orientation of the gonad in relation to the body axis were observed while imaging the ovaries in the context of the intact embryo (Fig. 1B, top, and Supplemental Fig. S4). Despite these changes, we still used the terms *ventral* and *dorsal*, in relation to the embryonic position, to identify different regions in the postnatal ovary (further information about orientation of the gonad during development and throughout the manuscript can be found in Supplemental Fig. S4 and Supplemental Movies S1 and S2).

We then studied the dynamics of transgene activation during the prepubertal period. The first detection of *Gdf9*-mCherry occurred at birth (Day 0) (Fig. 1, C and D0), whereas *Zp3*-AmCyan was initially observed at Day 4 for the majority of the animals (Fig. 1, C and D4). Interestingly, the first appearance of AmCyan was always restricted to a few oocytes located in the anterior-dorsal region of the ovary (Fig. 1C, dashed box). Because *Zp3* promoter activity is associated with transition to the primary follicle stage [26, 42], our data indicate that the first wave of follicle activation occurs within this specific region of the mouse ovary. During the neonatal period, the medullar region devoid of germ cells could still be identified in the dorsal side of the gonad (Fig. 1, C and D0–D6, all ovaries oriented with dorsal side up) while becoming less defined as larger follicles appear (Fig. 1, C and D12). Differences in follicle populations between dorsal and ventral regions of the ovary are discussed later.

In addition to localized patterns of follicle activation, follicle class-dependent expression patterns were observed. In primordial follicle oocytes, easily identified due to their small size and localization to the periphery, *Mvh*-EGFP and *Gdf9*-mCherry were the only fluorescent proteins detected (Fig. 1, D and E). In contrast, growing follicles had larger sizes and elevated levels of the reporter proteins (Fig. 1D and Supplemental Figs. S2 and S5). This indicates that the fluorescent signal changed according to the developmental stage of the oocyte, consistent with documented promoter activity [26, 28]. Additionally, a similar pattern of expression was observed when comparing the transgenes with the endogenous MVH, GDF9, and ZP3 proteins (Supplemental Fig. S2A). An exception was observed when the expressions of GDF9 and mCherry were compared in antral follicles, possibly because this transgenic line represents promoter activity and excludes any posttranscriptional regulation (Supplemental Fig. S2B). Importantly, we observed a complex and heterogeneous pattern of color within the same ovary, resulting from the overlay of the different reporter proteins with distinct expression levels, even among oocytes of the same follicle class, suggesting that each oocyte had its own fluorescent signal identity (Fig. 1, C–E, and Supplemental Fig. S5). Interestingly, variability within the same follicle class could be at least partially explained by age-related differences in oocyte expression levels (Supplemental Fig. S6). In fact, dramatic changes in the global intensity of the fluorescent signal occurred during the neonatal period, requiring the use of different imaging settings to detect the fluorescent proteins without reaching saturation of the images (double line in Fig. 1C separates images acquired with different imaging settings). Ovarian images acquired with the same exposure times can be found in Supplemental Figure S6A. Although variability in the fluorescent signal and the extent of activation was recognized between individual animals and litters, the spatial pattern of activation, with the first growing follicles appearing in the anterior-dorsal region, was similar in all the mice analyzed.

Altogether, we observed that the fluorescent profile of the oocytes changed with the developmental stage of the germ cells, validating the follicle class-dependent expression pattern and revealing new data regarding the region of first follicle activation.

Germ Cell Meiotic Entry Starts on the Ventral Region of the Mouse Ovary

The initial characterization of the triple transgenic mouse revealed that follicle activation in the neonatal mouse ovary was restricted to the anterior-dorsal region of the gonad (Fig. 1C, dashed box). Because it is well-established that germ cells enter meiosis in an anterior-to-posterior wave [3–6], we collected embryonic ovaries from transgenic mice to study the relationship between the onset of meiosis, follicle formation, and follicle activation, taking into account the ovarian anatomy. Thus, we examined the expression and localization of OCT4, STRA8, and MVH, which denote germ cells before, during, or independent of the meiotic entry, respectively [3, 38, 39]. At 12.5 dpc, no evidence of meiosis was found for the large majority of the gonads: OCT4 was uniformly distributed, and STRA8 expression was absent (Fig. 2). By 13.5 dpc, however, an anterior-to-posterior gradient could be detected in the ventral region, with depletion of OCT4 (Fig. 2i) and expression of STRA8 (Fig. 2ii) in the anterior region of the ovary. Surprisingly, in the dorsal region of the same 13.5-dpc ovary, the expression of STRA8 was restricted to very few germ cells, whereas OCT4 was expressed throughout this region, suggesting that the dorsal ovarian region has a later onset of meiosis. Despite the late onset, the dorsal region of the ovary also underwent meiosis, as evidenced by depletion of OCT4 (Fig. 2iii) and presence of STRA8 (Fig. 2iv) at 14.5 dpc. Slight variation between meiotic extension into the dorsal region could be observed in different animals and litters (Supplemental Fig. S7), but the early onset in the anterior-ventral region was observed in all the ovaries analyzed. Altogether, our data show, to our knowledge for the first time, that the onset of meiosis in the mouse ovary not only

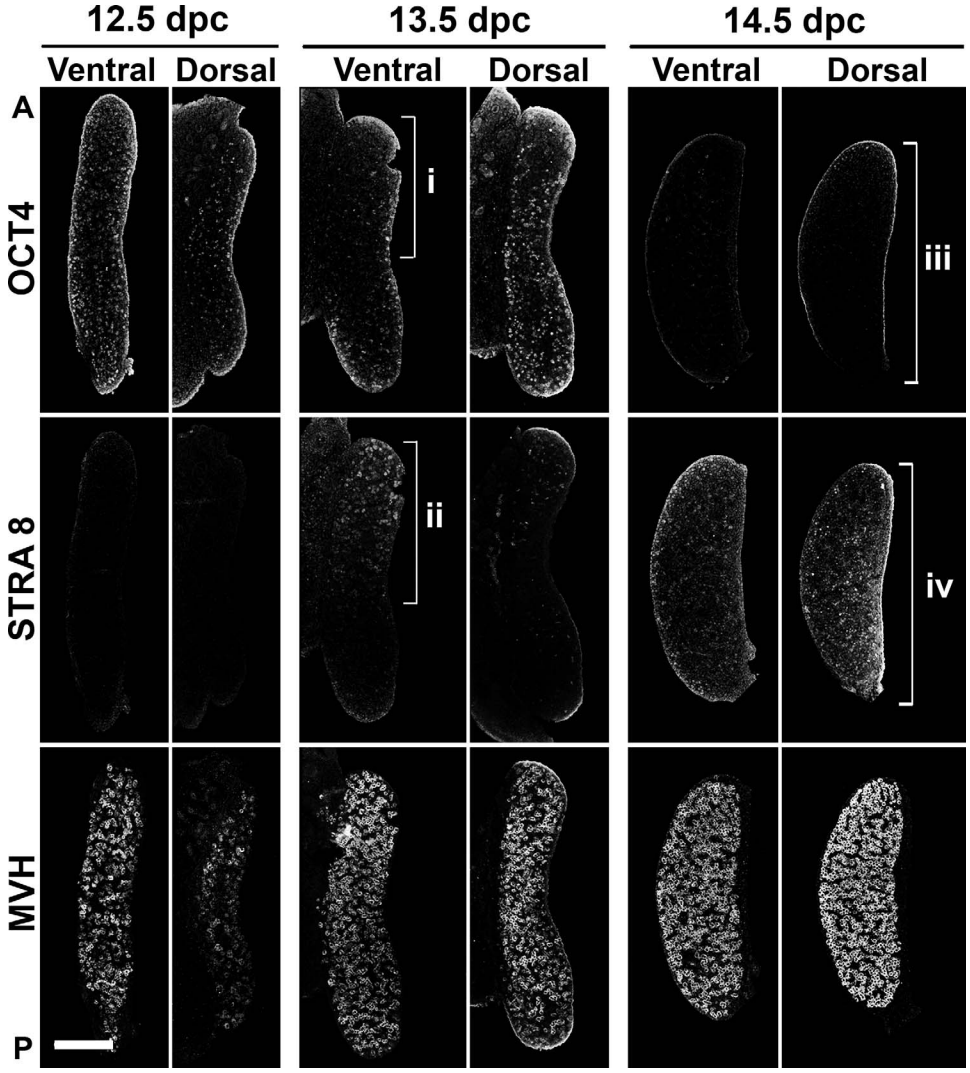

FIG. 2. Timing of meiosis entry differed between ventral and dorsal regions of the mouse ovary. Meiosis onset was visualized using immunofluorescence assay in serial sections with OCT4, STRA8, and MVH antibodies, allowing detection of germ cells before, during, and independent of the meiotic entry, respectively. Early onset of meiosis in the anterior-ventral region at 13.5 dpc as visualized by the depletion of OCT4 (i) and expression of STRA8 (ii) is shown. At 14.5 dpc, the dorsal region of the ovary also showed evidence of meiosis (iii and iv). Note the uniform distribution of germ cells in both regions of the gonad, visualized with MVH immunofluorescence assay. 12.5 dpc, n = 11; 13.5 dpc, n = 15; 14.5 dpc, n = 9. A, anterior; P, posterior. Bar = 200 μm.

occurs differentially in the anterior-posterior regions of the ovary but also in the dorsal-ventral regions.

First Individual Follicles Appear in the Anterior-Dorsal Region of the Mouse Ovary

The observation that the first wave of follicle activation occurred in the dorsal region of the ovary (Fig. 1C, dashed box) contrasts with the early meiosis entry occurring ventrally (Fig. 2). To understand these contrasting observations, we explored where the first individual follicles were formed. In mouse, follicle formation through nest breakdown is well characterized in the neonatal period; however, individual follicles are already present in the medulla at birth [44]. Thus, we analyzed ovaries during late embryonic development to explore the anatomic location of the first follicles formed, using MVH and FOXL2 as germ cell and granulosa cell lineage markers [24, 38], respectively. Consistent with Figure 1B, the specification of cortex and medulla could be seen at 16.5 dpc, with absence of germ cells (labeled with MVH) in the central area of the dorsal ovarian region (Fig. 3A, arrow). Interestingly, even before the specification of the medulla, a higher density of cells expressing FOXL2 could be found in the dorsal region at 14.5 dpc (Fig. 3A, arrowhead). FOXL2-labeled cells were not restricted to the ovarian medulla but were also around the germ cell clusters in the ventral region (Fig. 3Bii), and by 18.5 dpc, FOXL2-positive cells surrounded the first follicles formed in the dorsal region (Fig. 3Biv). Furthermore, the immunodetection of the basal lamina protein laminin, which delimits germ cell cords or individual follicles [45], also supported the notion that follicle formation was restricted to the dorsal region at 18.5 dpc (Fig. 3, A [double arrowheads] and C). We observed that even within the dorsal region of the ovary, geographic differences in development could be identified between the center and the periphery of the gonad. Specifically, whereas germ cells (labeled using the oocyte marker p63 [46]) toward the surface remained enclosed in clusters (Fig. 3, Cii and Civ), germ cells in the medulla formed individual follicles, especially in the anterior region (Fig. 3, Ciii and Cv). Altogether, we observed that the first individual follicles formed were located in the anterior-dorsal region of the 18.5-dpc ovary, the same region where the first growing follicles were detected in the

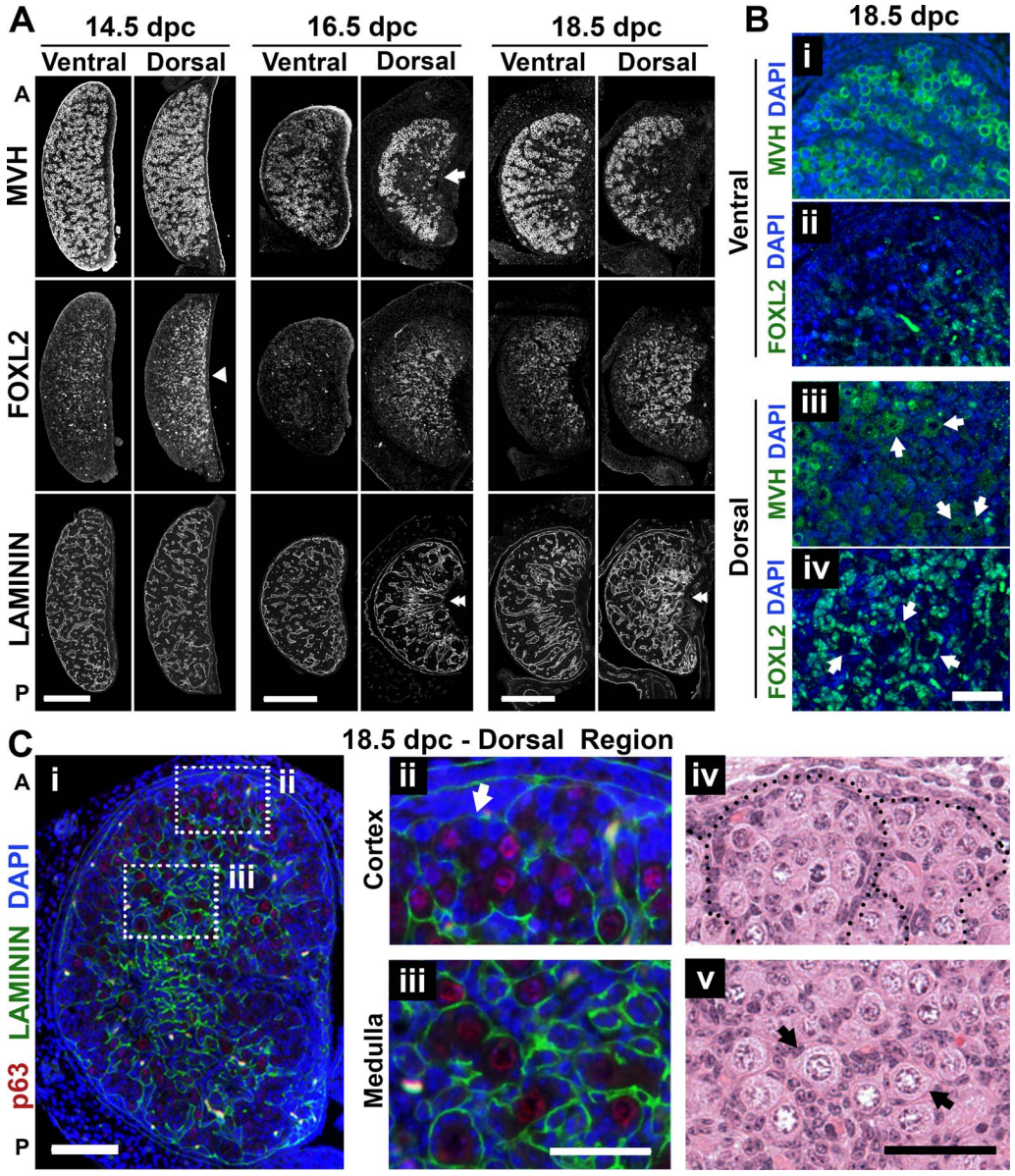

FIG. 3. Timing of individual follicle formation differed between ventral and dorsal regions of the mouse ovary. **A**) Differences between dorsal and ventral ovarian regions identified using immunofluorescence assay with MVH (germ cell), FOXL2 (pregranulosa), and laminin (basal lamina) antibodies in serial sections. Arrow highlights the specification of the medulla at 16.5 dpc. Arrowhead shows higher density of FOXL2-expressing cells in the dorsal region even before specification of the medulla. Double-arrowheads highlight dorsal-ventral differences in laminin organization. 14.5 dpc, n = 9; 16.5 dpc, n = 7; 18.5 dpc, n = 9. Bar = 200 μm. **B**) Individual follicle formation at 18.5 dpc was restricted to the dorsal region of the ovary, visualized using MVH (green; i and iii) and FOXL2 (green; ii and iv). Arrows represent individual primordial follicles. The images in i/ii and iii/iv are adjacent sections separated by 5 μm. Bar = 50 μm. **C**) Spatial differences in development between the center and the periphery of the dorsal region at 18.5 dpc (i) along with details of the germ cell clusters at the periphery (ii and iv) and individual follicles in the center (iii and v). Arrows highlight the presence of individual follicles. Red, p63 (oocyte nucleus); green, laminin; blue, DAPI. A, anterior; P, posterior. Bar = 100 μm (i) and 50 μm (ii–v).

neonatal ovary (identified based on their fluorescent profile), indicating that the distribution of follicles in the neonatal ovary is a consequence of embryonic development.

Embryonic Differences in Geography of Follicle Formation Influence the Developmental Status of the Germ Cell Throughout the Prepubertal Period

To determine if the distinct timing of embryonic follicle formation translated into postnatal spatial differences in follicle growth, we used confocal microscopy to monitor the different follicle populations in the surface of dorsal and ventral regions of the same ovary. Consistent with the observations at 18.5 dpc, growing follicles were observed on the dorsal region, predominantly, but not solely, in the anterior-dorsal region highlighted by the boxes in Figure 4A. In contrast, a higher number of primordial follicle oocytes were visible in the ventral region (Fig. 4A). In agreement with our observations, a nonrandom distribution of growing follicles was previously observed in rat ovaries [47] but not further investigated at the time. Interestingly, many primordial follicles on the ovarian surface remain organized in groups that resemble cord-like structures even after individualization (Fig. 4A, arrows). Because confocal imaging restricted the detection of the transgenes to the ovarian surface, we performed immunofluorescence assay with MVH antibody and evaluated follicle

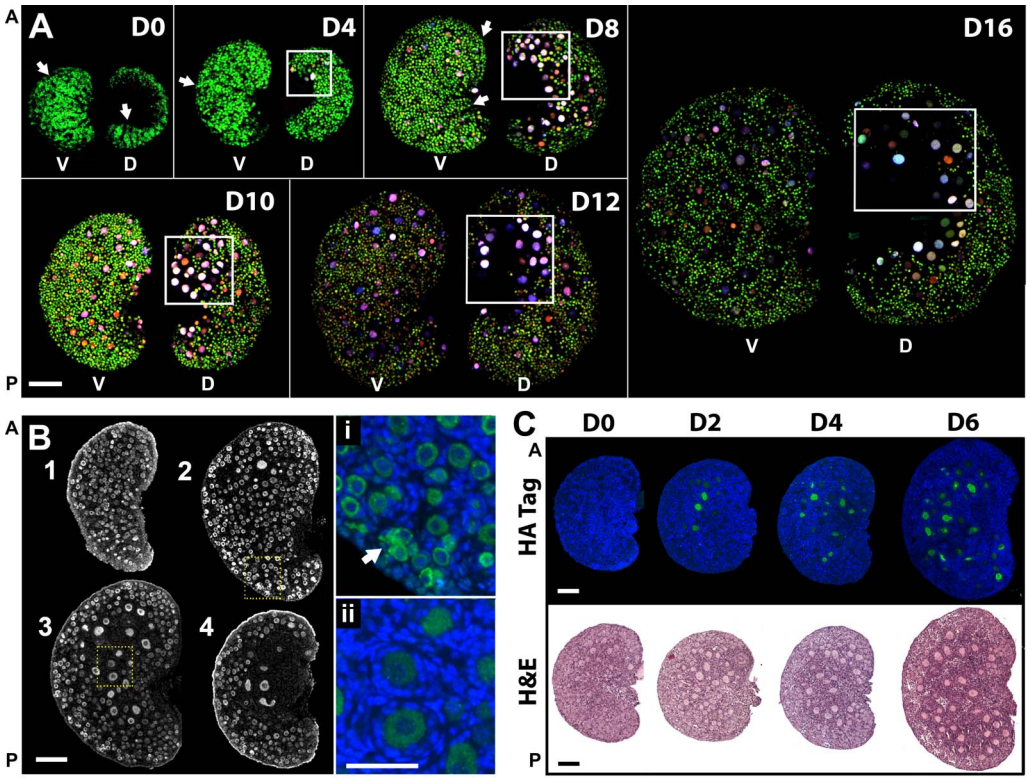

FIG. 4. Differential follicle development in ventral and dorsal ovarian regions is conserved throughout the prepubertal period. **A**) Maximum projection of confocal z-stack images revealed different oocyte populations on the surface of the two ovarian regions. Boxes highlight regions with elevated number of growing follicles (anterior-dorsal). Arrows exemplify follicle distribution resembling cord-like structures. The same imaging settings were used except Day 0 and Day 4, which required lower laser power for EGFP detection. Ventral (V) and dorsal (D) regions of the same ovary, rotated horizontally, are shown. Scale bars are approximated because images represent three-dimensional projections; n = 5 for each time point. Bar = ~200 μm. **B**) Geographic differences in follicle development in the same ovary. Immunofluorescence assay with MVH antibody in a 4-day-old mouse ovary in serial sections 45 μm apart (n = 6). Arrow shows region where ovarian nest remains. Highlighted areas are expanded on i and ii. 1, ventral; 4, dorsal. Green, MVH; blue, DAPI. Bar = 100 μm and 50 μm (i and ii). **C**) Gradual expansion of the ovarian region containing growing follicles; n = 6–10 for each represented time point. Green, HA tag; blue, DAPI; H&E, hematoxylin and eosin staining. A, anterior; P, posterior. Bar = 100 μm.

organization at different depths from the ovarian surface. We confirmed that most primordial follicles were localized in the ventral region of the ovarian cortex and were completely absent from the medulla, which exclusively contained growing follicles (Fig. 4B). Notably, the first primary and secondary follicles were present in the interface between cortex and medulla, whereas some germ cells on the surface of the ovary were still organized in nests (Fig. 4, Bi and Bii), reinforcing the concept that the initiation of follicle growth is not stochastic and that the trigger for follicle activation is related with geographic location in the ovary.

Primordial follicle recruitment during the pubertal period has been reported to occur gradually, contrasting with the synchrony of follicle activation described for the first wave of folliculogenesis [23]. Interestingly, we observed that the number of activated follicles in the dorsal region increased progressively as the mice aged (Days 0–6), represented by differences in follicle size in growing follicles expressing HA (tagged with AmCyan, driven by *Zp3* promoter) (Fig. 4C). This gradual recruitment created spatial organization as the area containing growing follicles expanded from a restricted medullar anterior-dorsal region into the periphery of the gonad and suggested asynchrony in follicle growth within the first wave of activation. This observation raises the question of which follicles should be included as first wave and suggests that the concept needs to be further specified.

In summary, we observed that distinct follicle formation patterns between dorsal and ventral regions of the embryonic ovary resulted in spatial differences in the ability to initiate follicle growth throughout the prepubertal period.

DISCUSSION

In the present study, we generated the first reporter mouse in which three fluorescent proteins are used simultaneously to follow follicle development. These animals showed normal folliculogenesis and expressed the fluorescent proteins in a follicle class-dependent pattern, consistent with the results of previous studies using the same promoters independently [26, 28]. The complexity in terms of color combinations in individual follicles suggests that germ cells are regulated autonomously rather than being part of a homogeneous pool. The differences in signal between primordial and growing follicles showed that the first activated follicles were located in the anterior-dorsal region of the ovary. The localization of these follicles in the anterior region led us to explore whether their activation correlated with the onset of meiosis, as described by the production line hypothesis [10]. Interestingly, the present study showed, to our knowledge for the first time, that the ventral side of the ovary has an earlier onset of meiosis, suggesting that the timing of meiotic entry might not be the main factor to induce follicle recruitment because the follicles first formed and activated were present in the dorsal region. Therefore, the present study does not support the production

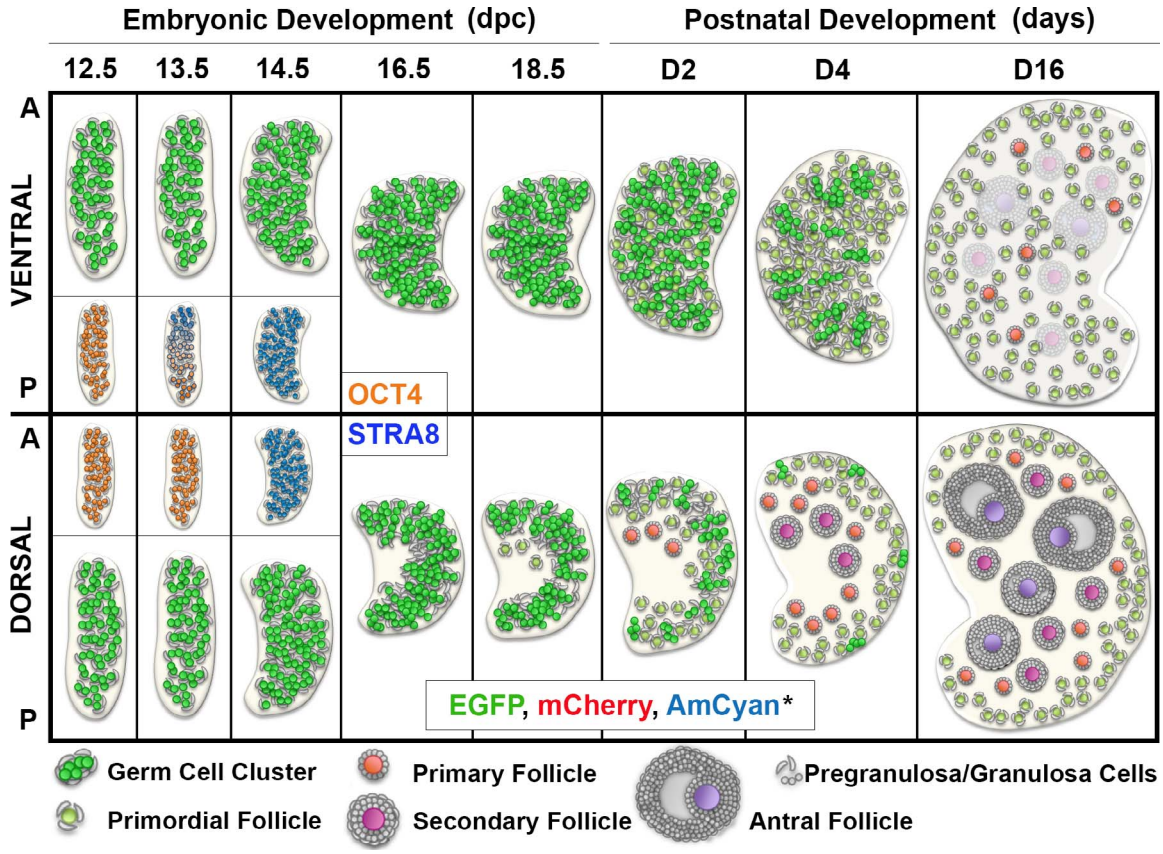

FIG. 5. Schematics of developmental events in the ventral and dorsal ovarian regions during the embryonic period and first wave of follicle activation. Early onset of meiosis in the ventral region is represented in the insert (OCT4 and STRA8). First primordial follicles were observed at 18.5 dpc at the interface between cortex and medulla in the anterior-dorsal region of the ovary, the area where the first cohort of growing follicles appear during the first week of postnatal development. In contrast, during this same period, germ cells in the ventral region of the ovary are still breaking the nest and forming individual follicles. The area containing growing follicles expands gradually during the postnatal period, occupying the whole medullar area of the dorsal region of the ovary. Altogether, our data indicated that the first wave of follicle activation follows a predictable anatomic pattern resulting from regional differences in timing of follicle formation. *Color resulting from the overlay of the three fluorescent proteins is represented. A, anterior; P, posterior.

line hypothesis; however, because possible germ cell rearrangements are not taken into account, the influence of the meiotic onset cannot be completely excluded. A tracing study using an inducible reporter mouse line (such as inducible *Stra8*) will be required to prove that oocytes do not move or are not passively shifted between regions during the development of the gonad.

Perhaps more intriguingly, our results suggest that the differentiation of cortical and medullar regions may have a greater impact in defining where the first follicle activation wave occurs. In accordance with this hypothesis, spatial differences in meiotic entry exist between mouse (anterior-to-posterior wave) and human (starting in the medulla and spreading radially to the cortex) [48, 49]. The first individual follicles, however, appear in the corticomedullar interface in both species, suggesting a common mechanism determined by a local factor, structure, or somatic cell population in the medulla. Few studies have explored the molecular mechanisms controlling specification toward cortex and medulla and their importance for normal ovarian development and functionality. Culture in vitro [50] and reaggregation experiments [51] were used to test the ability of the embryonic ovary to differentiate cortex from medulla, resulting in impaired development of early embryonic gonads or global recruitment to growth [50, 51]. It has been suggested that the specification of the medulla occurs due to selective apoptosis of medullar oocytes [52]; however, a recent study points to the gradual invasion of mesonephros-derived somatic cells as the driving force for the formation of ovarian cords and individual follicles [53]. Other studies reported molecular regionalization of the early mouse ovary, with particular focus on the distinct somatic cell populations present in different areas [54, 55]. This somatic cell regionalization becomes particularly relevant when taking into account the recent study showing that granulosa cells can initiate primordial follicle activation [56]. Importantly, granulosa cells arise from the surface epithelium in two distinct waves, one before sexual differentiation and contributing to medullary located follicles and another recruited perinatally and contributing to cortically located primordial follicle formation in the neonatal period [24, 57]; thus, granulosa cell origins and correct differentiation may have an important role maintaining the balance between primordial follicle quiescence and activation. Other factors that may contribute to the regionalization of primordial follicle formation and activation include the influence of secreted factors through the vasculature (because the major blood vessels are normally found in the medulla of the dorsal region of the ovary) [58, 59] and the influence of the rete ovarii (implicated in both meiosis and follicle formation) [60, 61]. In summary, we hypothesize that the germ cell asymmetry in development between ovarian regions may result from how the germ cells wrap around and interact with the newly formed microenvironment of the medulla in the dorsal region of the ovary. Further studies are required to clarify the molecular mechanisms regulating follicle

formation in the embryonic gonad and to explain why it occurs mainly in the anterior-dorsal region of the ovary.

The gradual and asynchronous expansion of the region containing growing follicles during the neonatal period (Fig. 4C) suggests that recruitment of immediately adjacent follicles may occur as a consequence of differences in the timing of follicle formation or through the influence of signals released during the embryonic period or by growing follicles in close proximity. The follicles from the first wave of activation may then control the consecutive rounds of follicle activation by impacting the growth of neighboring follicles [62], establishing a hierarchy of primordial follicle activation. The activated primordial follicles can then be selected by the endocrine action of follicle-stimulating hormone and luteinizing hormone, thus linking the hormone-independent and hormone-dependent phases of follicle development, which is the underpinning responsible for reproductive cyclicity and longevity [23, 63].

Altogether, our data indicate that recruitment of a restricted cohort of follicles during the first wave of follicle activation is likely achieved by an early onset of follicle formation in the dorsal region of the ovary, allowing some follicles to initiate growth whereas others in the ventral region remain quiescent (Fig. 5). Continuing to explore how the embryonic organization of the gonad and the intercommunication between follicles affects ovarian functionality will be essential to understand how the balance between quiescence, activation, growth, and germ cell loss is established and maintained in the ovary, which has implications for reproductive aging and premature ovarian failure in humans.

ACKNOWLEDGMENT

The genetically engineered mice were generated with the assistance of Northwestern University (NU) Transgenic and Targeted Mutagenesis Laboratory (partially supported by NIH grant CA60553 to the Robert H. Lurie Comprehensive Cancer Center). Traditional sequencing services were performed at the NU Genomics Core Facility. Imaging work was performed at the NU Cell Imaging Facility (generously supported by NCI CCSG P30 CA060553 awarded to the Robert H Lurie Comprehensive Cancer Center). We thank Dr. Richard M. Schultz, Dr. Austin J. Cooney, and Dr. Diego Castrillon for generously providing the plasmids containing the *Zp3, Gdf9,* and *Mvh* promoters, respectively, and GenScript for performing subcloning of the *Mvh* promoter. We thank Dr. Lynn Doglio for crucial advice during mouse design and Dr. Leong Chew for imaging assistance. We acknowledge Megan M. Romero and Keisha M. Barreto (the NU Ovarian Histology Core: P01HD021921) for sectioning of our samples and Kelly Whelan for animal care assistance. We also thank Dr. Danielle Maatouk for important comments on the manuscript.

REFERENCES

1. Baker TG. Radiosensitivity of mammalian oocytes with particular reference to the human female. Am J Obstet Gynecol 1971; 110:746–761.
2. Kerr JB, Myers M, Anderson RA. The dynamics of the primordial follicle reserve. Reproduction 2013; 146:R205–R215.
3. Menke DB, Koubova J, Page DC. Sexual differentiation of germ cells in XX mouse gonads occurs in an anterior-to-posterior wave. Dev Biol 2003; 262:303–312.
4. Bullejos M, Koopman P. Germ cells enter meiosis in a rostro-caudal wave during development of the mouse ovary. Mol Reprod Dev 2004; 68: 422–428.
5. Bowles J, Knight D, Smith C, Wilhelm D, Richman J, Mamiya S, Yashiro K, Chawengsaksophak K, Wilson MJ, Rossant J, Hamada H, Koopman P. Retinoid signaling determines germ cell fate in mice. Science 2006; 312: 596–600.
6. Koubova J, Menke DB, Zhou Q, Capel B, Griswold MD, Page DC. Retinoic acid regulates sex-specific timing of meiotic initiation in mice. Proc Natl Acad Sci U S A 2006; 103:2474–2479.
7. Pepling ME, Spradling AC. Mouse ovarian germ cell cysts undergo programmed breakdown to form primordial follicles. Dev Biol 2001; 234: 339–351.
8. Adhikari D, Liu K. Molecular mechanisms underlying the activation of mammalian primordial follicles. Endocr Rev 2009; 30:438–464.
9. Reddy P, Zheng W, Liu K. Mechanisms maintaining the dormancy and survival of mammalian primordial follicles. Trends Endocrinol Metab 2010; 21:96–103.
10. Henderson SA, Edwards RG. Chiasma frequency and maternal age in mammals. Nature 1968; 218:22–28.
11. Polani PE, Crolla JA. A test of the production line hypothesis of mammalian oogenesis. Hum Genet 1991; 88:64–70.
12. Hirshfield AN. Heterogeneity of cell populations that contribute to the formation of primordial follicles in rats. Biol Reprod 1992; 47:466–472.
13. Tease C, Fisher G. Further examination of the production-line hypothesis in mouse fetal oocytes. I. Inversion heterozygotes. Chromosoma 1986; 93: 447–452.
14. Speed RM, Chandley AC. Meiosis in the fetal mouse ovary. II. Oocyte development and age-related aneuploidy. Does a production line exist? Chromosoma 1983; 88:184–189.
15. Wandji SA, Srsen V, Voss AK, Eppig JJ, Fortune JE. Initiation in vitro of growth of bovine primordial follicles. Biol Reprod 1996; 55:942–948.
16. Meredith S, Doolin D. Timing of activation of primordial follicles in mature rats is only slightly affected by fetal stage at meiotic arrest. Biol Reprod 1997; 57:63–67.
17. Rowsey R, Gruhn J, Broman KW, Hunt PA, Hassold T. Examining variation in recombination levels in the human female: a test of the production-line hypothesis. Am J Hum Genet 2014; 95:108–112.
18. Tease C, Fisher G. Further examination of the production-line hypothesis in mouse fetal oocytes. II. T(14; 15)6Ca heterozygotes. Chromosoma 1989; 97:315–320.
19. Byskov AG, Skakkebaek NE, Stafanger G, Peters H. Influence of ovarian surface epithelium and rete ovarii on follicle formation. J Anat 1977; 123: 77–86.
20. Konishi I, Fujii S, Okamura H, Parmley T, Mori T. Development of interstitial cells and ovigerous cords in the human fetal ovary: an ultrastructural study. J Anat 1986; 148:121–135.
21. Sawyer HR, Smith P, Heath DA, Juengel JL, Wakefield SJ, McNatty KP. Formation of ovarian follicles during fetal development in sheep. Biol Reprod 2002; 66:1134–1150.
22. McGee EA, Hsu SY, Kaipia A, Hsueh AJ. Cell death and survival during ovarian follicle development. Mol Cell Endocrinol 1998; 140:15–18.
23. Zheng W, Zhang H, Gorre N, Risal S, Shen Y, Liu K. Two classes of ovarian primordial follicles exhibit distinct developmental dynamics and physiological functions. Hum Mol Genet 2014; 23:920–928.
24. Mork L, Maatouk DM, McMahon JA, Guo JJ, Zhang P, McMahon AP, Capel B. Temporal differences in granulosa cell specification in the ovary reflect distinct follicle fates in mice. Biol Reprod 2012; 86:37.
25. Suzuki H, Dann CT, Rajkovic A. Generation of a germ cell-specific mouse transgenic CHERRY reporter, *Sohlh1-mCherryFlag*. Genesis 2013; 51: 50–58.
26. Lan ZJ, Xu X, Cooney AJ. Differential oocyte-specific expression of Cre recombinase activity in *GDF-9-iCre*, *Zp3cre*, and *Msx2Cre* transgenic mice. Biol Reprod 2004; 71:1469–1474.
27. Svoboda P. Cloning a transgene for transgenic RNAi in mouse oocytes. Cold Spring Harb Protoc 2009; doi:10.1101/pdb.prot5134.
28. Gallardo T, Shirley L, John GB, Castrillon DH. Generation of a germ cell-specific mouse transgenic Cre line, *Vasa-Cre*. Genesis 2007; 45:413–417.
29. McLean AC, Valenzuela N, Fai S, Bennett SA. Performing vaginal lavage, crystal violet staining, and vaginal cytological evaluation for mouse estrous cycle staging identification. J Vis Exp 2012; e4389.
30. Nagy AGM, Vintersten K, Behringer R. Manipulating the Mouse Embryo: A Laboratory Manual. Cold Spring Harbor, NY: Cold Spring Harbor Laboratory Press; 2003:234–236 and 293–294.
31. Pedersen T, Peters H. Proposal for a classification of oocytes and follicles in the mouse ovary. J Reprod Fertil 1968; 17:555–557.
32. Bristol-Gould SK, Kreeger PK, Selkirk CG, Kilen SM, Mayo KE, Shea LD, Woodruff TK. Fate of the initial follicle pool: empirical and mathematical evidence supporting its sufficiency for adult fertility. Dev Biol 2006; 298:149–154.
33. Kurita T. Developmental origin of vaginal epithelium. Differentiation 2010; 80:99–105.
34. John GB, Gallardo TD, Shirley LJ, Castrillon DH. Foxo3 is a PI3K-dependent molecular switch controlling the initiation of oocyte growth. Dev Biol 2008; 321:197–204.
35. Reddy P, Liu L, Adhikari D, Jagarlamudi K, Rajareddy S, Shen Y, Du C, Tang W, Hamalainen T, Peng SL, Lan ZJ, Cooney AJ, et al. Oocyte-specific deletion of *Pten* causes premature activation of the primordial follicle pool. Science 2008; 319:611–613.
36. Jagarlamudi K, Liu L, Adhikari D, Reddy P, Idahl A, Ottander U, Lundin

E, Liu K. Oocyte-specific deletion of *Pten* in mice reveals a stage-specific function of PTEN/PI3K signaling in oocytes in controlling follicular activation. PLOS ONE 2009; 4:e6186.
37. de Vries WN, Binns LT, Fancher KS, Dean J, Moore R, Kemler R, Knowles BB. Expression of Cre recombinase in mouse oocytes: a means to study maternal effect genes. Genesis 2000; 26:110–112.
38. Noce T, Okamoto-Ito S, Tsunekawa N. Vasa homolog genes in mammalian germ cell development. Cell Struct Funct 2001; 26:131–136.
39. Toyooka Y, Tsunekawa N, Takahashi Y, Matsui Y, Satoh M, Noce T. Expression and intracellular localization of mouse *Vasa*-homologue protein during germ cell development. Mech Dev 2000; 93:139–149.
40. McGrath SA, Esquela AF, Lee SJ. Oocyte-specific expression of growth/differentiation factor-9. Mol Endocrinol 1995; 9:131–136.
41. Dong J, Albertini DF, Nishimori K, Kumar TR, Lu N, Matzuk MM. Growth differentiation factor-9 is required during early ovarian folliculogenesis. Nature 1996; 383:531–535.
42. Philpott CC, Ringuette MJ, Dean J. Oocyte-specific expression and developmental regulation of ZP3, the sperm receptor of the mouse zona pellucida. Dev Biol 1987; 121:568–575.
43. Wassarman PM, Jovine L, Litscher ES. Mouse zona pellucida genes and glycoproteins. Cytogenet Genome Res 2004; 105:228–234.
44. Peters H. The development of the mouse ovary from birth to maturity. Acta Endocrinol (Copenh) 1969; 62:98–116.
45. Lee VH, Britt JH, Dunbar BS. Localization of laminin proteins during early follicular development in pig and rabbit ovaries. J Reprod Fertil 1996; 108:115–122.
46. Suh EK, Yang A, Kettenbach A, Bamberger C, Michaelis AH, Zhu Z, Elvin JA, Bronson RT, Crum CP, McKeon F. p63 protects the female germ line during meiotic arrest. Nature 2006; 444:624–628.
47. Hirshfield AN, DeSanti AM. Patterns of ovarian cell proliferation in rats during the embryonic period and the first three weeks postpartum. Biol Reprod 1995; 53:1208–1221.
48. Anderson RA, Fulton N, Cowan G, Coutts S, Saunders PT. Conserved and divergent patterns of expression of DAZL, VASA and OCT4 in the germ cells of the human fetal ovary and testis. BMC Dev Biol 2007; 7:136.
49. Wilhelm D, Yang JX, Thomas P. Mammalian sex determination and gonad development. Curr Top Dev Biol 2013; 106:89–121.
50. Byskov AG, Guoliang X, Andersen CY. The cortex-medulla oocyte growth pattern is organized during fetal life: an in-vitro study of the mouse ovary. Mol Hum Reprod 1997; 3:795–800.
51. Nicholas CR, Haston KM, Pera RA. Intact fetal ovarian cord formation promotes mouse oocyte survival and development. BMC Dev Biol 2010; 10:2.
52. Maatouk DM, Capel B. Sexual development of the soma in the mouse. Curr Top Dev Biol 2008; 83:151–183.
53. Hummitzsch K, Irving-Rodgers HF, Hatzirodos N, Bonner W, Sabatier L, Reinhardt DP, Sado Y, Ninomiya Y, Wilhelm D, Rodgers RJ. A new model of development of the mammalian ovary and follicles. PLOS ONE 2013; 8:e55578.
54. Chen H, Palmer JS, Thiagarajan RD, Dinger ME, Lesieur E, Chiu H, Schulz A, Spiller C, Grimmond SM, Little MH, Koopman P, Wilhelm D. Identification of novel markers of mouse fetal ovary development. PLOS ONE 2012; 7:e41683.
55. Rastetter RH, Bernard P, Palmer JS, Chassot AA, Chen H, Western PS, Ramsay RG, Chaboissier MC, Wilhelm D. Marker genes identify three somatic cell types in the fetal mouse ovary. Dev Biol 2014; 394:242–252.
56. Zhang H, Risal S, Gorre N, Busayavalasa K, Li X, Shen Y, Bosbach B, Brannstrom M, Liu K. Somatic cells initiate primordial follicle activation and govern the development of dormant oocytes in mice. Curr Biol 2014; 24:2501–2508.
57. Harikae K, Miura K, Shinomura M, Matoba S, Hiramatsu R, Tsunekawa N, Kanai-Azuma M, Kurohmaru M, Morohashi K, Kanai Y. Heterogeneity in sexual bipotentiality and plasticity of granulosa cells in developing mouse ovaries. J Cell Sci 2013; 126:2834–2844.
58. Maatouk DM, Mork L, Hinson A, Kobayashi A, McMahon AP, Capel B. Germ cells are not required to establish the female pathway in mouse fetal gonads. PLOS ONE 2012; 7:e47238.
59. Yao HH, Matzuk MM, Jorgez CJ, Menke DB, Page DC, Swain A, Capel B. *Follistatin* operates downstream of *Wnt4* in mammalian ovary organogenesis. Dev Dyn 2004; 230:210–215.
60. Byskov AG. Does the rete ovarii act as a trigger for the onset of meiosis? Nature 1974; 252:396–397.
61. Byskov AG, Lintern-Moore S. Follicle formation in the immature mouse ovary: the role of the rete ovarii. J Anat 1973; 116:207–217.
62. Durlinger AL, Kramer P, Karels B, de Jong FH, Uilenbroek JT, Grootegoed JA, Themmen AP. Control of primordial follicle recruitment by anti-Mullerian hormone in the mouse ovary. Endocrinology 1999; 140:5789–5796.
63. Edson MA, Nagaraja AK, Matzuk MM. The mammalian ovary from genesis to revelation. Endocr Rev 2009; 30:624–712.
64. Nicholls PK, Harrison CA, Gilchrist RB, Farnworth PG, Stanton PG. Growth differentiation factor 9 is a germ cell regulator of Sertoli cell function. Endocrinology 2009; 150:2481–2490.